Cyclic stress-strain curves and internal friction of steel at ultrasonic frequencies

A. PUŠKÁR

A new interpretation of some characteristics of material push-pull loaded at a frequency of 23 kHz can be evaluated by measuring the internal friction and elasticity modulus defect at different strain amplitudes. It is possible to obtain interesting relations describing the material's cyclic microplasticity response. The paper presents some basic relationships between the 'plastic' internal friction, elasticity modulus defect, hysteresis loop area, plastic strain amplitude and the cyclic deformation hardening coefficient, for low carbon steel with different grain sizes.

KEYWORDS: ultrasonics, internal friction, steel

List of symbols

A	displacement amplitude
E	elasticity modulus
H_p	hysteresis loop shape factor
Q^{-1}	internal friction of specimen
Q_w^{-1}	internal friction of whole system
Q_u^{-1}	internal friction of system without specimen
Q_p^{-1}	'plastic' internal friction
Q_c^{-1}	internal friction at ϵ_c
Q_ϵ^{-1}	internal friction at some value of ϵ
$U_a(U_{ar})$	applied voltage (at resonance)
U_A	voltage from capacitance measuring of displacement amplitude
$U_{pu}(U_{pur})$	pickup voltage (at resonance)
U_T	voltage from strain gauge
W	total supplied energy
ΔW_p	dissipated energy during one loading cycle
d_1, d_2, d_3	grain size of steel
$f(f_r)$	frequency (at resonance)
n	cyclic hardening coefficient
$\Delta E/E$	elasticity modulus defect
ϵ	strain amplitude in middle section of specimen
$\epsilon_M, \epsilon_T, \epsilon_A$	strain amplitude evaluated by Mason's calculation, by strain gauge and by displacement amplitude measuring
ϵ_{at}	total strain amplitude
ϵ_{ae}	elastic strain amplitude
ϵ_{ap}	plastic strain amplitude
ϵ_c	critical strain amplitude
λ	wavelength
σ_a	stress amplitude
$E_x, \epsilon_{aex}, \epsilon_{apx}, \epsilon_{ax}, f_{rx}$	values of E, ϵ_{ae}, ϵ_{ap}, σ_a, f_r at some strain amplitude higher than ϵ_c

Introduction

A control factor in the accumulation of fatigue damage is plastic strain amplitude. Direct measuring of the plastic strain amplitude component from the total strain amplitude at ultrasonic loading frequencies is very complicated or even impossible. Recently it was assumed[1] that all the mechanical energy transferred to the specimen during cyclic loading is transformed to an increase in solid state internal energy by an increase in dislocation density, vacancy concentration, etc, and more than 98 % of supplied energy can be changed into heat. The measuring of specimen temperature increase by thermocouple,[1] by a weak layer of cholesteric liquid coating[2] or analytically solving different approximations of the hysteresis loop area equation,[3] shows a way of estimating the plastic strain amplitude contribution of the total strain amplitude in different places of simple shaped waveguides made from different materials. There are basic possibilities for evaluating microplastic deformation distribution along the waveguides.

The author is with the Department of Mechanical Technology, University of Transport and Telecommunications, 010 88 Žilina, Czechoslovakia. Paper received 2 February 1981. Revised 26 June 1981.

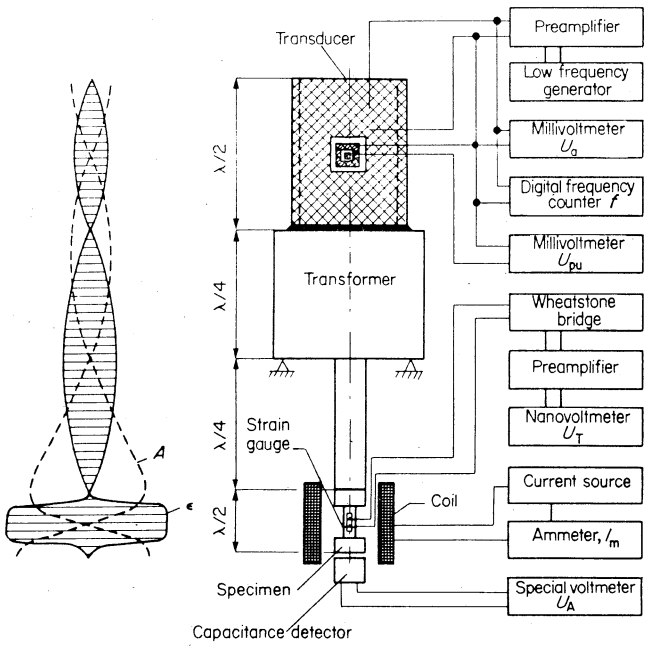

Fig. 1 Full resonance system with schematic view of apparatus. Distribution of displacement amplitude A and strain amplitude ϵ along resonance system

Measuring internal friction and elasticity modulus defect in the material's microplastic deformation region gives more useful information about the interaction of high-energy ultrasound with solid state materials. The hysteresis loop area and shape are integral characteristics of these processes. Evaluation of hysteresis loop parameters after saturation of the material property changes developed by cyclic deformation makes it possible to find cyclic stress-strain curves and to estimate material fatigue durability at ultrasonic frequency loading.

Experimental equipment and method

The resonance system[4,5,6] shown in Fig. 1 consists of a driving transducer, stub transformer, and the dumb-bell-shaped specimen. The transducer is a piezoelectric PZT ceramic in the form of a hollow cylinder (external diameter 38 mm, internal diameter 32 mm) with silver electrodes on both the external and internal cylindrical surfaces. The transducer is cemented with epoxy resin to the stub transformer made from one piece of A1SVF titan alloy with an upper diameter of 54 mm and lower diameter of 12 mm. The specimen is held on the end of the transformer by a screw joint. The heads of the specimen have a diameter of 12 mm and the middle section has a diameter of 3 mm. Each part of the system was dimensioned to resonate longitudinally at 23 kHz.

The current (Fig. 1) from the low frequency generator (from 16 to 25 kHz) passes through a preamplifier to the external and internal conductive layers of the transducer. The applied voltage U_a is measured by a millivoltmeter, and the current frequency f by a digital frequency counter. At the mid-length of the transducer are two small square areas on opposite sides of the external surface which were isolated to serve as detectors of strain amplitude by measuring the pickup voltage U_{pu} on another millivoltmeter.

From the arrangement of the resonance system, basic knowledge of propagation of longitudinal ultrasonic waves,[7] and from the fact that force and velocity are continuous at each interface, it follows that the successive reductions in cross-sectional area from the transducer via the transformer to the specimen result in corresponding increases in displacement amplitude A as well as strain amplitude ϵ along the resonance system (Fig. 1). Maximum strain amplitude takes place in the middle of the specimen and is nearly uniform. It was assumed that in the transducer, stub transformer, and heads of the specimen only fully elastic reaction could take place but in the middle of the specimen microplastic reaction of materials with ultrasonic loading also occurs.[4-6]

It has been shown[4,6] that there is a linear dependence between pickup voltage U_{pu} and strain amplitude ϵ_M in the middle section of the specimen, and so

$$\epsilon_M = \xi U_{pu} \tag{1}$$

where ξ is constant for the resonance system. Equation (1) has been checked by positioning a strain gauge with a high frequency response directly on the specimen. The electrical signal leads to a Wheatstone bridge, and a preamplifier and is measured by a frequency selective nanovoltmeter. The displacement amplitude A of the free end of the specimen was measured by a frequency-tuned capacitance detector which measured the voltage $U_A(\sim A)$ by special apparatus. The relation between A and strain amplitude ϵ_A can be found in the literature.[8] From a statistical treatment of strain amplitude values measured by a different procedure at U_a from 0.1 to 150 V we find good agreement between ϵ_M, ϵ_T and ϵ_A for different U_{pu}, especially at $U_{pu} \geqslant 0.3$ V.

For evaluation of internal friction and elasticity modulus defect we often need to ignore the magnetomechanical part of internal friction. We used an electrical coil with a single-phase current source, with the current I_m measured by an ammeter.

The internal friction of the whole system Q_w^{-1} can be calculated from

$$Q_w^{-1} = \left(\frac{K U_{ar}}{f_r U_{pur}}\right)_w = \left(\frac{\Delta f_{r3dB}}{f_r}\right)_w, \tag{2}$$

where K is a constant and Δf_{r3dB} is a 3 dB separation of resonance frequency, that is, the difference between the frequencies at which the amplitude of oscillation falls to $A_r/\sqrt{2}$, where A_r, U_{ar} and U_{pur} are values of A, U_a and U_{pu} at resonance frequency.

The internal friction of the specimen Q^{-1} can be calculated by the equation

$$Q^{-1} = k_1 Q_w^{-1} - k_2 Q_u^{-1}, \tag{3}$$

where k_1 and k_2 are constants connected with the influence of effective masses and mechanical resistance of the whole resonance system and Q_u^{-1} is internal friction which can be calculated by (2) for the resonance system without the specimen.

Loading the specimen with strain amplitude $\epsilon_x \geqslant \epsilon_c$, where ϵ_c is the critical amplitude[9] we can find the fall in resonance frequency f_r for some value of f_{rx}. The elasticity modulus defect $\Delta E/E$ can be calculated by the equation

$$\frac{\Delta E}{E} = \eta \frac{2(f_r - f_{rx})}{f_r} \tag{4}$$

where η is a constant depending on the ratio of the effective masses and stiffnesses of the whole resonance system and the specimen.

The advantage of this kind of equipment and measuring method is that it is quite simple to record U_{ar}, U_{pur} and f_r (or f_{rx}) and it is possible to obtain the internal friction characteristics of different materials at strain amplitudes from 5×10^{-7} to 3×10^{-3} with or without magnetic field as well as independently measuring the internal friction and evaluating the elasticity modulus defect characteristics over a wide interval of strain amplitudes.

Experimental material and procedure

The low carbon unalloyed steel consisted of 0.07 % C, 0.006 % N, 0.27 % Mn, 0.03 % Si, 0.013 % P, 0.018 % S and 0.07 % Cr. After heat treatment the bars had ferritic grain size $d_1 = 0.022 \pm 0.004$ mm, $d_2 = 0.29 \pm 0.045$ mm or $d_3 = 0.62 \pm 0.085$ mm. The dumb-bell shaped specimen in the middle section was carefully machined and mechanically polished, then annealed at 200°C for 30 min in an argon atmosphere and slowly cooled in the furnace, and finally chemically polished.

Specimens were attached to the resonance system described and cyclically loaded at the frequency of 23 kHz with a total strain amplitude ranging from 5×10^{-6} to 4×10^{-4} at room temperature and in the presence of a magnetic field intensity of 1.9×10^4 A m^{-1}. Simultaneously for each experimental point the internal friction Q^{-1}, elasticity modulus defect $\Delta E/E$ and total strain amplitude ϵ_{at}, were measured for 100 s at constant ϵ_{at}. We assumed that 2.3×10^6 loading cycles was enough for saturation of material property changes over the strain amplitude interval mentioned above.

Results

The internal friction level at $\epsilon_{at} = 5 \times 10^{-6}$ depends on the ferritic grain size (Fig. 2). An increase in steel grain size causes a rise in internal friction. There are also differences in the behaviour of Q^{-1} against ϵ_{at} for steel with different grain sizes in the amplitude-dependent region of internal friction. Exceeding ϵ_c causes a strong increase in elasticity modulus defect. The value of critical strain amplitude is a function of ferritic grain size (Table 1). Changes in elasticity modulus defect at the increasing values of the total strain amplitude are more pronounced for steel with a larger grain size than for fine grained steel.

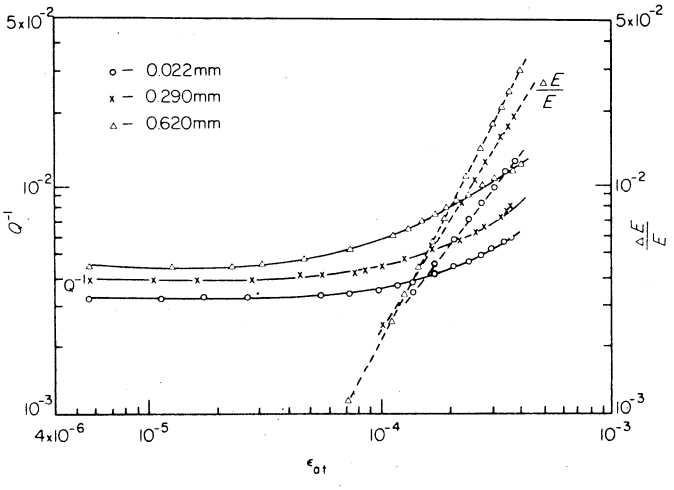

Fig. 2 Dependence of internal friction Q^{-1} (continuous lines) and elasticity modulus defect $\Delta E/E$ (broken lines) on total strain amplitude for steel with different grain sizes

Table 1. Microplastic characteristics response factors and exponents for steel with different grain sizes (d)

d [mm]	ϵ_c	b	n	κ [MPa]	c	g	l
0.022	1.3×10^{-4}	1.313	0.410	9700	2.30	1.092	3.260
0.290	1.0×10^{-4}	1.661	0.357	4400	2.60	0.790	3.610
0.620	7.3×10^{-5}	1.967	0.320	2700	2.97	0.732	3.917

For evaluation of the stress amplitude σ_a in the middle section of the specimen for each experimental point, that is, for each total strain amplitude value, this approximation can be used (Fig. 3a). In the fully elastic region of cyclic loading $\sigma_a = E\,\epsilon_{ae}$, where ϵ_{ae} is an elastic strain amplitude and E is the elasticity modulus of the specimen which is also characterized by the basic resonance frequency of the system f_r. In the elastic-plastic region, at some point x, the stress amplitude $\sigma_{ax} = E_x(\epsilon_{aex} + \epsilon_{apx}) = E_x\,\epsilon_{atx}$, where ϵ_{ap} is the plastic strain amplitude and E_x is the elasticity modulus of the specimen which is characterized by the resonance frequency of the system, f_{rx} at the point x, when $\epsilon_{at} > \epsilon_c$. Then, $E_x = E - \Delta E_x$, where ΔE_x is the elasticity modulus change as a consequence of the specimen's microplastic deformation.

From the approximation valid at the start of the cyclic microplastic region we may derive:

$$\sigma_a = \epsilon_{at}(E - \Delta E) = \epsilon_{at}E\left(1 - \frac{\Delta E}{E}\right), \tag{5}$$

$$\epsilon_{ap} = \epsilon_{at} - \epsilon_{ae} = \epsilon_{at} - \frac{\sigma_a}{E} = \epsilon_{at}\frac{\Delta E}{E}. \tag{6}$$

In the region $\epsilon_{at} > \epsilon_c$ an increase in elasticity modulus defect with rising total strain amplitude is more pronounced for steel with large grain size than for fine grained steel. From Fig. 2 it is clear that experimental points are linear with log-log coordinates. Thus

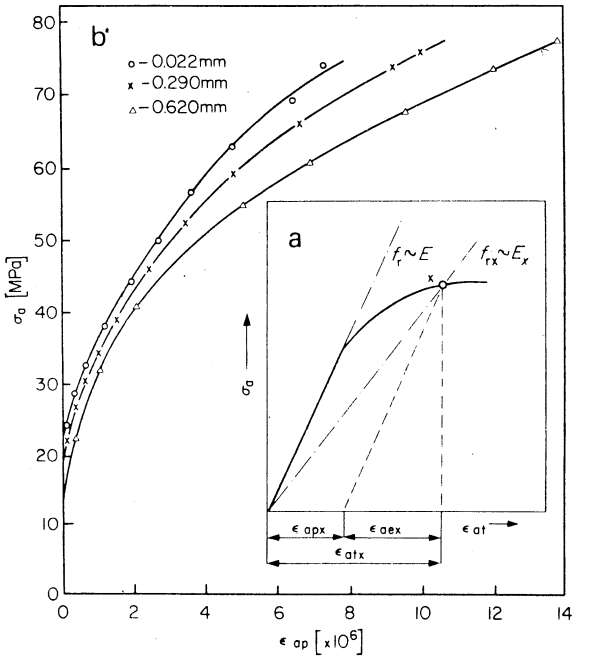

Fig. 3 a — Scheme for approximation; and b — cyclic stress-strain curves for steel with different grain sizes

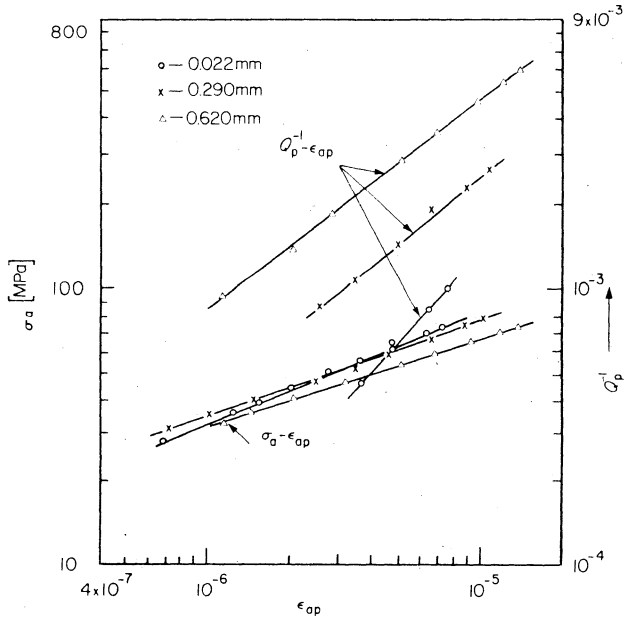

Fig. 4 Dependence of the stress amplitude σ_a or 'plastic' internal friction Q_p^{-1} on plastic strain amplitude ϵ_{ap} for steel with different grain sizes

$$\frac{\Delta E}{E} = B\,\epsilon_{at}^{b} \tag{7}$$

where B and b are structurally sensitive constants, which increase with grain size, as shown in Table 1 for factor b.

The approximation and derived equations (5) and (6) make it possible to find the relation between stress amplitude σ_a and plastic strain amplitude ϵ_{ap} for each experimental point. When we applied the approximation, for steel with different grain sizes, we obtained typical cyclic stress-strain curves (Fig. 3b). In log-log coordinates (Fig. 4) we can see linear relations which are analytically expressed by the equation

$$\sigma_a = \kappa\,\epsilon_{ap}^{n} \tag{8}$$

where κ and n are structurally sensitive constants (Table 1). An increase in ferritic grain size of steels from 0.022 to 0.62 mm causes a decrease in the cyclic hardening coefficient n from 0.41 to 0.32 and a decrease in the factor κ from 9700 MPa to 2700 MPa.

In the region where $\epsilon_{at} > \epsilon_c$ we may also express the relation ϵ_{ap} against ϵ_{at} (Fig. 5) by the equation

$$\epsilon_{ap} = C\,\epsilon_{at}^{c} \tag{9}$$

where C and c are structurally sensitive constants (Table 1). To a first approximation the factor $c \sim 1/n$. From (9) and from Fig. 5 it can be seen that applying ϵ_{at} develops a higher value of plastic strain amplitude in steel with large grain size than in fine grained steel.

It is useful to separate internal friction at $\epsilon_{at} > \epsilon_c$ and to label part as 'plastic' internal friction, that is, $Q_p^{-1} = Q_\epsilon^{-1} - Q_c^{-1}$, where Q_ϵ^{-1} is internal friction at some value of $\epsilon_{at} > \epsilon_c$ and Q_c^{-1} is internal friction at[9] $\epsilon_{at} = \epsilon_c$. From the experiments (Fig. 4) verification of the equation

$$Q_p^{-1} = G\,\epsilon_{ap}^{g} \tag{10}$$

is clear, where G and g are constants dependent on ferritic grain size (Table 1). A similar value of applied ϵ_{at} for steel with larger grain size causes a higher dissipation of mechanical energy which can be connected with easier movement and origination of dislocation segments than in the fine grained steel.

The 'plastic' internal friction Q_p^{-1} is the ratio of the dissipated energy during one cycle of loading ΔW_p and total supplied energy[10] W, where $\Delta W_p = H_p\,\sigma_a\,\epsilon_{ap}$ or $W = \frac{1}{2}E\,\epsilon_{at}^2$. Then

$$Q_p^{-1} = \frac{\Delta W}{2\pi W} = \frac{H_p\,\sigma_a\,\epsilon_{ap}}{E\,\epsilon_{at}^2} \tag{11}$$

where H_p is a hysteresis loop shape factor at $\epsilon_{at} > \epsilon_c$. From this we can find the interesting result that the plastic strain amplitude is a function of the cyclic deformation factor, that is,

$$\epsilon_{ap} = \left(\frac{\pi Q_p^{-1} E}{H_p \kappa}\,\epsilon_{at}^2\right)^{\frac{1}{n+1}} \tag{12}$$

The hysteresis loop area increases with a rise in plastic strain amplitude loading. Inserting (7) and (9) into (11) gives

$$\Delta W_p = L\,\epsilon_{at}^{l} \tag{13}$$

which is confirmed for steel with different grain sizes in Fig. 5. The factor L and the exponent l increase with an increase in ferritic grain size, (Table 1).

In the strain amplitude region considered no one factor or exponent basically dependent on ferritic grain size fulfils Hull-Petch's relation.

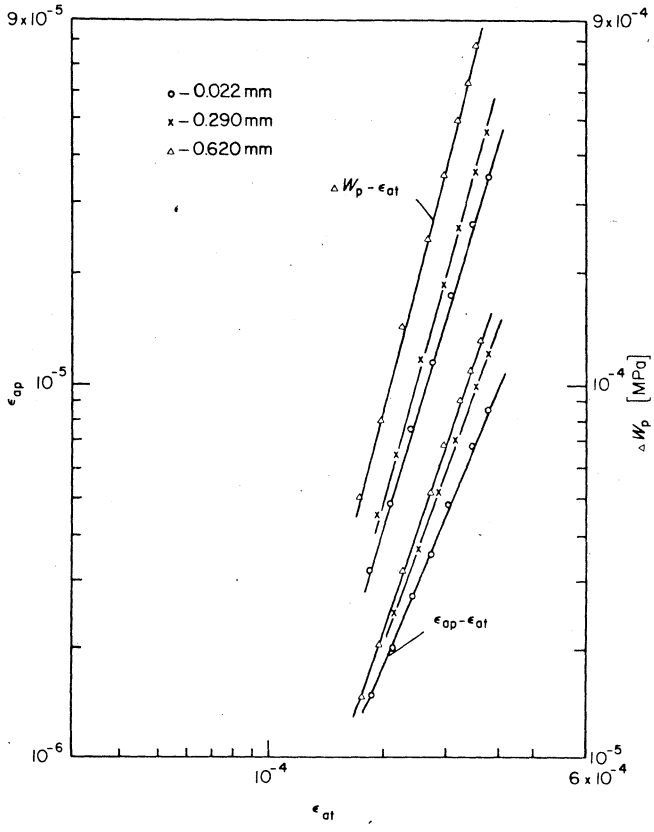

Fig. 5 Dependence of the plastic strain amplitude ϵ_{ap} or hysteresis loop area ΔW_p on total strain amplitude ϵ_{at} for steel with different grain sizes

Discussion

An increase in internal friction level as well as a decrease in critical strain amplitude with increasing grain size of iron or steel have been explained for ultrasonic frequency loading[5] and also for ordinary frequency loading.[11]

The basic equations for plastic response on cyclic loading at 23 kHz are the same as for the ordinary loading frequency (8) but with a different value of factor κ and exponent n. For example, with low carbon steel loaded at 70 Hz the factor κ = 853 MPa and n = 0.156 have been found.[12] The higher values of κ and n obtained at 23 kHz showed an increase in material response against cyclic microplastic deformation at high frequency loading.

The plastic strain amplitude ϵ_{ap} at 23 kHz proves to be only a few percent of the total strain amplitude. A similar observation can be found in the case of copper loading at 21 kHz.[2] When the loading frequency is 70 Hz the part ϵ_{ap} of total strain amplitude is many times higher.[12] It can be understood that some ϵ_{at} develops a more pronounced microplastic effect in the material at low frequency than at ultrasonic frequency loading. These differences can be a consequence of: the limited time for dislocation of segments moving under the stress amplitude; worse conditions for stress peak relaxation; extremely localized microplastic deformation; a decrease in microplastic deformation activation volume,[13] the increasing of material response against deformation; as well as the consequence of an increase in the cyclic deformation hardening coefficient on the application of high frequency loading.

The influence of grain boundary on some cyclic microplastic characteristics of low carbon steel has been found to be smaller at a loading frequency of 23 kHz than with static deformation or a low frequency cyclic loading. We assume that in the region of strain amplitude examined the dislocations preferentially interacted among themselves and with other structural obstacles in more cases than with grain boundaries.

The stress amplitude, 'plastic' internal friction, elasticity modulus defect, hysteresis loop area and other cyclic microplastic characteristics are an exponential function of the strain amplitude value. Thus it is true to say that the value of strain amplitude plays a very important role in the fatigue damage accumulation process.

Conclusions

Stress amplitude, 'plastic' internal friction, elasticity modulus defect, and hysteresis loop area are exponential functions of the plastic strain amplitude for low carbon steel with different grain sizes at the loading frequency of 23 kHz.

The plastic strain amplitude proves to be only a few percent of the total strain amplitude when the material is loaded at 23 kHz.

The independent measuring of internal friction and elasticity modulus defect at a total strain amplitude makes it possible to evaluate the plastic strain amplitude as well as the cyclic stress-strain curves in the region of very small total strain amplitude (less than 5×10^{-4}) at a loading frequency of 23 kHz.

An increase of ferritic grain size when applying the total strain amplitude causes an increase in the plastic strain amplitude, 'plastic' internal friction, and hysteresis loop area.

References

1 **Bajons, P., Weiss, B.** *Ultrasonics* **13** (1975) 248
2 **Wielke, B., Stanzl, S.** *Ultrasonics* **14** (1976) 227
3 **Wielke, B.** *Phys. Stat. Sol. (a)* **23** (1974) 237
4 **Mason, W.P.** in Microplasticity, ed. C.J. McMahon, Jr. Advances in Materials Research, Vol. 2, Wiley, New York (1968) 287
5 **Jon, M.C., Mason, W.P., Beshers, D.N.** *J. Appl. Phys.* **47** (1976) 2337
6 **Puškár, A.** *Ultrasonics* **15** (1977) 124
7 **Puškár, A.** Fyzikálne, metalurgické a technologické aspekty využitia intenzívneho ultrazvuku, Veda Bratislava (1977)
8 **Bajons, P., Kromp, W.** *Ultrasonics* **16** (1978) 213
9 **Golovin, S.A., Puškár, A.** *Kovov. Mater.*, **16** (4) (1978) 426
10 **Troščenko, V.T.** Ustalost' i neuprugost' metallov, Naukova dumka Kijev (1971)
11 **Burdett, C.F.** *Phil Mag.* **24** (1971) 1459
12 **Klesnil, M., Lukáš, P.** Únava kovových materiálu při mechanickém namáhaní, Academia Praha (1975)
13 **Puškár, A.** *Kovov. Mater.*, **18** (6) (1980) 629